Numerical Simulations of Large-scale Solar Magnetic Fields*

C. R. DeVore,[A] *N. R. Sheeley, Jr,*[B] *J. P. Boris,*[A]
T. R. Young, Jr[A] *and K. L. Harvey*[C]

[A] Laboratory for Computational Physics, Code 4040,
Naval Research Laboratory, Washington, DC 20375, U.S.A.
[B] E.O. Hulburt Center for Space Research,
Naval Research Laboratory, Washington, DC 20375, U.S.A.
[C] Solar Physics Research Corporation,
4720 Calle Desecada, Tucson, AZ 85718, U.S.A.

Abstract

We have solved numerically a transport equation which describes the evolution of the large-scale magnetic field of the Sun. Data derived from solar magnetic observations are used to initialize the computations and to account for the emergence of new magnetic flux during the sunspot cycle. Our objective is to assess the ability of the model to reproduce the observed evolution of the field patterns. We discuss recent results from simulations of individual active regions over a few solar rotations and of the magnetic field of the Sun over sunspot cycle 21.

1. Introduction

Leighton (1964) proposed a quantitative model for the evolution of the large-scale solar magnetic field at the photosphere in which the field is sheared by differential rotation and dispersed by diffusion. In his theory, the diffusion results from the random walk of the photospheric plasma and its frozen-in magnetic field in the constantly shifting pattern of supergranulation cells. He showed that this model provides a natural explanation for the decay of active-region flux, the formation of unipolar magnetic regions, and the reversal of the Sun's global dipole field over the course of the sunspot cycle.

In recent years, evidence has mounted that a poleward meridional surface flow is present on the Sun (Duvall 1979; Howard 1979; Howard and LaBonte 1981; LaBonte and Howard 1982; Topka *et al.* 1982). We have incorporated a meridional flow into Leighton's transport model (Sheeley *et al.* 1983; DeVore *et al.* 1984) in order to study the relative effects of diffusion, differential rotation, and meridional flow on large-scale photospheric magnetic structures. In this paper we describe our recent efforts to simulate the decay phase of several individual active regions and to reproduce the main characteristics of the mean magnetic field of the Sun during sunspot cycle 21.

* Paper presented at the R. G. Giovanelli Commemorative Colloquium, Part II, Tucson, Arizona, 17–18 January 1985.

2. Flux Transport Model

The evolution equation for the radial component of the large-scale magnetic field at the photosphere $B(\theta, \phi, t)$ is (Leighton 1964; Devore *et al.* 1984)

$$\frac{\partial B}{\partial t} + \frac{1}{R}\frac{1}{\sin\theta}\frac{\partial}{\partial\theta}\left(v(\theta)\,B\,\sin\theta\right) + \omega(\theta)\frac{\partial B}{\partial\phi}$$

$$+ \frac{\kappa}{R^2}\frac{1}{\sin\theta}\frac{\partial}{\partial\theta}\left(\sin\theta\frac{\partial B}{\partial\theta}\right) + \frac{\kappa}{R^2}\frac{1}{\sin^2\theta}\frac{\partial^2 B}{\partial\phi^2} = S(\theta, \phi, t). \qquad (1)$$

The independent variables are the spherical polar angle θ, the azimuthal angle ϕ and the time t. The parameters of the transport model are the rotation rate $\omega(\theta)$, the meridional flow velocity $v(\theta)$, and the diffusion constant κ. The radius of the Sun is denoted by R. The quantity $S(\theta, \phi, t)$ is a source term representing the emergence of new active-region magnetic flux through the photosphere.

Equation (1) is a linear, inhomogenous transport equation on the surface of a sphere. We solve it using a fast Fourier transform along azimuths, and a combination of a flux-conserving convection algorithm and an implicit diffusion algorithm along meridians. This combination of techniques possesses excellent numerical stability and conservation properties.

In our studies of the decay of individual active regions we have used digital magnetic data collected at the National Solar Observatory at Kitt Peak (NSO/KP). We selected pairs of observations of each region in our sample, and simulated the evolution of the region from the earlier observation to the later one. The data at the earlier rotation were deposited onto the model grid as the initial flux distribution $B(\theta, \phi, t = 0)$. The data at the later rotation were directly compared against the solution $B(\theta, \phi, t = T)$ obtained by integrating equation (1) for $s \equiv 0$, where T is the time elapsed between the initial and final rotations.

In our studies of the mean solar magnetic field we have treated the newly emerged active regions as point bipoles, or doublets. Using photographic prints of the NSO/KP magnetograms, one of us (N.R.S.) has estimated the latitudes and longitudes of the centroids of positive and negative flux, and the total flux content, of approximately 2500 such sources of new photospheric flux which erupted in the interval 1976–84. Supplementing this source record is the NSO/KP synoptic map of the magnetic field for Carrington rotation (CR) 1646, which we used to initialize the simulations. Equation (1) was solved with these initial conditions $B(\theta, \phi, t = 0)$ and sources $S(\theta, \phi, t)$ to obtain the daily flux distribution $B(\theta, \phi, t)$. Averaging the line-of-sight component of this field over the earthward hemisphere, we derived the mean solar magnetic field $\langle B(t)\rangle$. This simulated field was then compared against Stanford Solar Observatory (SSO) measurements of the mean magnetic field of the Sun.

3. A Study of Individual Active Regions

We acquired digital magnetic data for several consecutive appearances near central meridian of each of seven prominent active regions. The selection of the regions was based on their relative isolation on the solar surface, their simple initial magnetic structure, and their distribution over the range of active solar latitudes. In Table 1 we list some basic data for these regions, including the Carrington rotation numbers for

Table 1. Basic data for seven prominent active regions

Tabulated for each of the seven bipolar magnetic regions are: the heliographic latitude and Carrington longitude of the centroid of total flux of the region at its first appearance near central meridian; the corresponding Carrington rotation number and date; and the Carrington rotation numbers for which pairs of observations were suitable for deposition into and comparison with the simulation model

Pair no.	Initial latitude	Initial longitude	Initial rotation	Initial date	Deposition rotation	Comparison rotation
1	5 N	310	1631	8/3/75	1632	1633
2	10 N	175	1622	12/13/74	1623	1624
3	20 S	15	1649	12/30/76	1649	1650
4					1651	1652
5	20 S	205	1656	6/25/77	1656	1657
6					1658	1659
7	30 S	210	1650	1/14/77	1650	1651
8					1650	1652
9					1651	1652
10	30 N	5	1650	1/27/77	1650	1651
11					1650	1652
12					1651	1652
13	40 S	160	1651	2/14/77	1651	1652
14					1651	1653
15					1652	1653

which pairs of observations were suitable for deposition into and comparison with the simulation model. Other combinations of deposition and comparison rotation numbers for several of the regions are possible in principle, but were ruled out in practice due to eruptions of additional flux within the region or to intermingling of the spreading flux of the region with nearby, pre-existing large-scale flux.

We determined best-fit values of the transport parameters—the rotation rate, the meridional flow velocity, and the diffusion constant—for each of the fifteen pairs of observations tabulated in Table 1. Our procedure was to substitute the expressions

$$\omega(\theta) = \omega_0 + \omega_2 \cos^2 \theta, \qquad v(\theta) = v_0 \sin 2\theta, \qquad \kappa = \kappa_0 \qquad \text{(2a,b,c)}$$

into equation (1), and to solve that equation to obtain the flux distribution at the comparison rotation. The coefficient of differential rotation in equation (2a) is the grand average for recurrent sunspots found by Newton and Nunn (1951), given by $\omega_2 = -2 \cdot 77$ deg.day^{-1}. The functional form for the meridional flow velocity was chosen for its smoothness, its antisymmetry across the equator, and its nulls at the solar poles. We self-consistently determined the convection constants ω_0 and v_0 by requiring the centroid of total flux of the simulated distribution to coincide with that of the observed distribution. As a measure of the ability of the model to emulate the Sun, we correlated the simulated and observed fluxes pixel by pixel. We determined the diffusion constant κ_0 as the numerical value of κ which maximizes this correlation coefficient.

The results are shown in Fig. 1, in which we have plotted as data points (a) the synodic rotation rate, (b) the meridional flow velocity, and (c) the diffusion constant for each of the simulation pairs, evaluated at the heliographic latitude of the centroid of total flux at the comparison rotation.
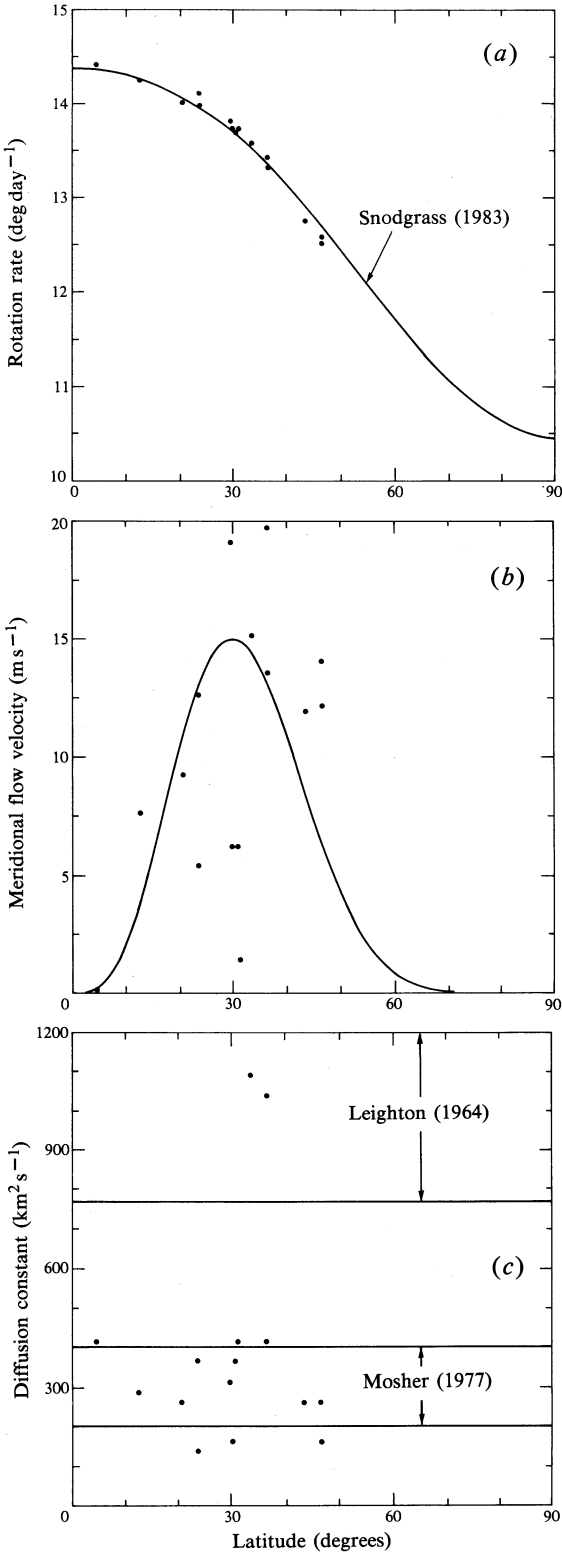
Fig. 1. Plotted are
(*a*) the synodic solar rotation rate,
(*b*) the meridional flow velocity,
(*c*) the diffusion constant
versus heliographic latitude.
Data points correspond to the
active-region simulation pairs
given in Table 1.
The curves are discussed
in Section 3.

The curve in the plot of rotation rate in Fig. 1*a* was taken from the recent work by Snodgrass (1983). He cross-correlated day-to-day observations of photospheric magnetic features as they rotated across the solar disc, and found

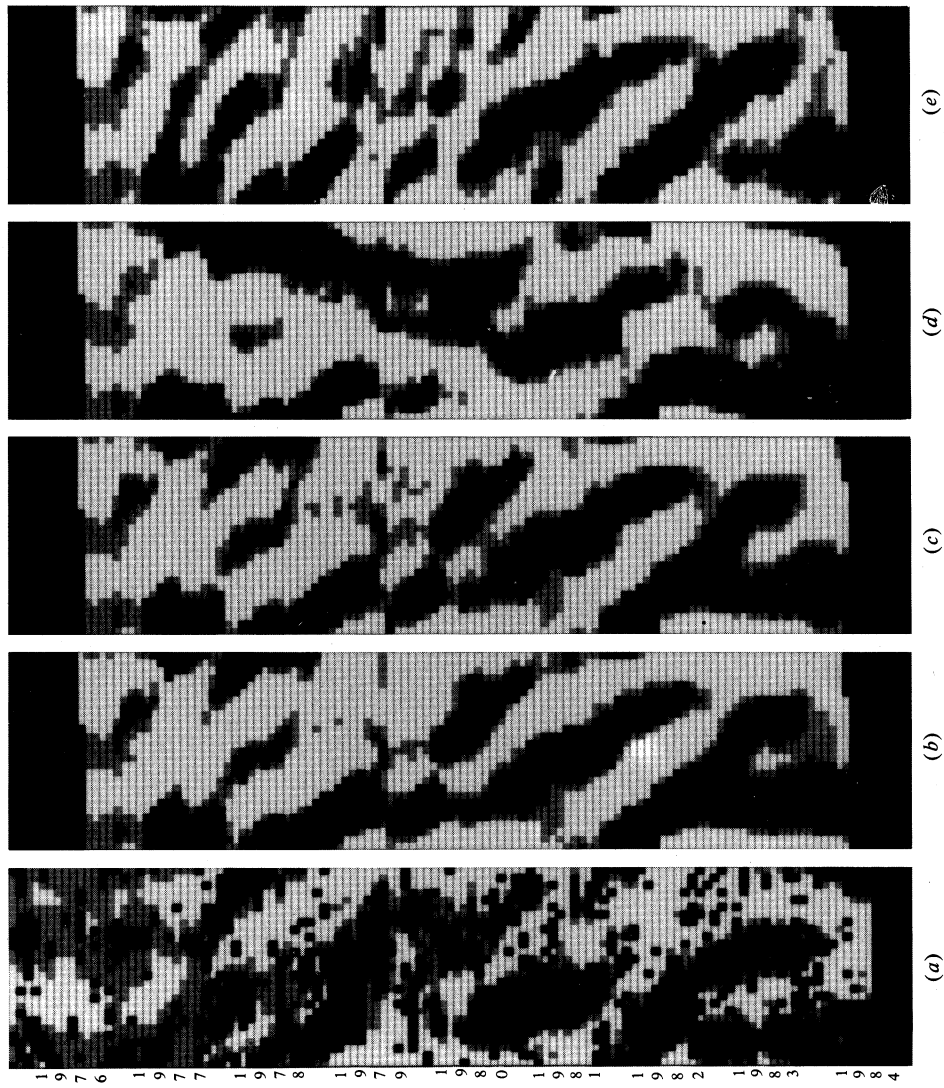$$\omega(\theta) = 14 \cdot 37 - 2 \cdot 30 \cos^2 \theta - 1 \cdot 62 \cos^4 \theta \ \mathrm{deg.day}^{-1}.$$

At sunspot latitudes, his rate is in close agreement with that found by Newton and Nunn (1951). The local rates which result from our model simulations are consistent with Snodgrass' measurements over the entire latitude range of the regions in our sample. The r.m.s. deviation of the individual points from his curve is $0 \cdot 12$ deg.day^{-1}, or roughly 1%.

In the plot of meridional flow velocities in Fig. 1*b*, a positive value indicates a poleward-directed flow in either hemisphere. The local velocities determined in the simulations are all nonnegative and lie in the range 0–20 m s^{-1}. These results agree in direction and magnitude with measurements of the meridional motions of the photospheric plasma (Duvall 1979; Howard 1979; LaBonte and Howard 1982), of surface magnetic fields (Howard and LaBonte 1981), and of Hα filaments (Topka *et al.* 1982). In contrast to the rotation rates from the simulations, however, the meridional flow velocities exhibit no simple variation with latitude, and the scatter in the local velocities is comparable with the velocities themselves. The curve shown is a 'nominal' profile which we use in the mean-field simulations, to be described in Section 4.

We indicate in the plot of the diffusion constant in Fig. 1*c* a portion of the range of values, 770–1540 km^2 s^{-1}, given originally by Leighton (1964), and the entire range of 200–400 km^2 s^{-1} estimated more recently by Mosher (1977). Leighton arrived at his estimate by calibrating the time of reversal of the polar magnetic fields in a model calculation of the sunspot cycle. Mosher measured the rate of areal spreading of a number of aging solar active regions using photographic prints of magnetograms. With two exceptions, the individual values obtained in our simulations lie within or adjacent to Mosher's range, scattered about a mean of 300 km^2 s^{-1} by ±50%. The two exceptions are associated with entries 10 and 11 in Table 1. That particular region emerged during CR 1650 as a pair of neighbouring bipolar structures. By CR 1651, it had evolved into a simple bipolar configuration. It is possible that some dynamical interaction not accounted for by the flux transport model significantly influenced the development of the region between rotations 1650 and 1651, and skewed the results for these two simulation pairs.

We have considered several possible sources of error in the determinations of the transport parameters. With regard to the data, the undetected emergence of additional flux in the region during the simulation interval cannot be ruled out. However, the amount of the new flux which could escape detection in our procedure is almost certainly too small to have a significant impact on the results. With regard to the method, random errors associated with the finite resolution of the computational mesh are estimated at $0 \cdot 05$ deg.day^{-1} for the rotation rates and 7 m s^{-1} for the meridional flow velocities, too small to account for all of the scatter in these two quantities. A change in the criterion for determining the diffusion constant, to the condition that the total surviving flux at the comparison rotation be the same for the simulated and observed fields, does not substantially reduce the scatter in the values obtained. Finally, with regard to the model, there is the possibility of the breakdown

Fig. 2. Plotted in a Bartels format are daily values of the mean solar magnetic field for the interval 1976–84. Stanford Solar Observatory data are displayed in (*a*), while simulation results for four sets of model parameters are displayed in (*b*)–(*e*).

or invalidity of the assumptions underlying it. Inspection of the simulated and observed flux distributions at the comparison rotation invariably reveals small-scale structure present in the observations which is absent in the simulations. This fact reflects the filamentary character of the photospheric magnetic field; only its spatially averaged, large-scale properties can be expected to be well represented by the flux transport model (cf. DeVore *et al.* 1984). It may be that the inability of the model to reproduce these small-scale features is responsible for much of the random scatter in our results.

4. A Study of the Mean Solar Magnetic Field

We have calculated daily values of the mean magnetic field of the Sun over the interval from September 1976 to June 1984 for several combinations of choices for the parameters in the transport equation. Our basic set of parameters for this study is the rotation rate found by Snodgrass (1983) given in Section 3, a null meridional flow velocity, and the maximum value for the diffusion constant estimated by Mosher (1977) of 400 $km^2 s^{-1}$. This set yields simulated mean-field patterns in substantial qualitative agreement with those observed. By varying the parameters in the basic set one at a time, we can identify signatures in the resulting patterns associated with each of the transport mechanisms.

The mean field over this extended interval of time is conveniently presented in a Bartels plot, in which the daily values of the field are arranged in a running calendar of 27-day 'months'. We code the field values using a grey scale, ranging from dark grey (negative polarity) through medium grey (field strength below $0 \cdot 1$ G) to light grey (positive polarity). Black indicates an absence of data. In Fig. 2*a* we show the SSO daily measurements, beginning on 10 January 1976 at the top left of the plot. In Fig. 2*b* we show the mean field calculated using our basic parameter set. While there clearly are detailed differences between these two plots, particularly in the fine structure apparent in the observations, the large-scale organization of the patterns is strikingly similar. The degree of agreement was rather surprising to us, in the light of our rough accounting of the sources of new flux.

The first variation on the basic parameter set which we consider is a doubling of the diffusion constant to 800 $km^2 s^{-1}$. This value lies at the lower end of Leighton's (1964) estimated range. The resulting mean field is shown in Fig. 2*c*. A comparison with the standard case reveals only minimal changes in the patterns. The dominant effect of the increased rate of diffusion is a general reduction in the field strengths. This reduction is evident, upon careful inspection, in the slight broadening of the neutral lines in the plot. A general weakening of the mean field is consistent with an increase in the rate of dispersal of the active-region flux, which reduces the time required for the flux to decay away.

Our second variation on the basic parameter set is a substitution of the rotation rate reported recently by Howard *et al.* (1984) for the Snodgrass (1983) rate. They measured the rotational motions of individual sunspots, and as a grand average found that

$$\omega(\theta) = 14 \cdot 52 - 2 \cdot 84 \sin^2 \theta \ \text{deg.day}^{-1}.$$

Use of this expression in the calculation leads to substantially different patterns in the mean field, as shown in Fig. 2*d*. The larger rotation rate at equatorial latitudes causes the field patterns to effectively undergo retrograde motion in the 27-day frame of the

Bartels plot. This direction of slant in the patterns does not appear in the plot of the SSO data. That the sunspot rotation rate is relatively unsuccessful in the mean-field simulations is perhaps not surprising. We might expect the primary contributors to the mean field to be the extended unipolar regions which form as active regions age, rather than the compact, young bipolar regions which contain sunspots.

The third and final variation that we discuss is the addition of a poleward meridional flow to the basic parameter set. Our assumed velocity profile, which reaches a peak of 15 m s^{-1} at 30° latitude, has been displayed in Fig. 1 *b*. We plot the resulting mean field in Fig. 2 *e*. The addition of meridional flow leads to a disruption in the continuity of the large-scale patterns and to a general increase in their slant. Both of these effects can be expected to follow from a rapid poleward motion of active-region flux. The increase in latitude of the flux reduces the line-of-sight component at Earth, thereby accelerating the weakening of its contribution to the mean field and shortening the patterns, and reduces the rate of rotation of the flux, thereby increasing the slant of the patterns in the 27-day Bartels frame.

Our initial attempts to simulate the mean magnetic field of the Sun have been successful to the extent that the large-scale organization of the patterns in the simulations and observations are in agreement. It seems clear that further progress in evaluating the model will require a more accurate and detailed accounting of the sources of new magnetic flux during the sunspot cycle. The effects of uncertainties in the diffusion constant are primarily quantitative in nature, determining the overall field strengths without greatly affecting the location of the magnetic neutral line. The effect of adding a meridional flow on the agreement between the simulated and observed mean field is rather ambiguous, improving it at some points and degrading it at others. At this time, discrepancies in the simulated field caused by uncertainties in the parameters or in the model itself cannot be unambiguously distinguished from those caused by inaccuracies in the properties of the sources.

5. Discussion

The results of the calculations discussed in this paper demonstrate the ability of the flux transport model to reproduce the global features of the solar magnetic field. At the same time, there is a conspicuous absence in the numerical simulations of the fine structure present in the observations. As we discussed in connection with the study of individual active regions, this may reflect an inescapable limitation to the validity of the model. Nevertheless, the model has clearly increased our qualitative understanding of magnetic fields on the Sun. We are just beginning to evaluate its potential to account with quantitative accuracy for the large-scale characteristics of those fields.

References

DeVore, C. R., Sheeley, N. R., Jr, and Boris, J. P. (1984). *Sol. Phys.* **92**, 1.

Duvall, T. L., Jr (1979). *Sol. Phys.* **63**, 3.

Howard, R. (1979). *Astrophys. J. Lett.* **228**, L45.

Howard, R., Gilman, P. A., and Gilman, P. I. (1984). *Astrophys. J.* **283**, 373.

Howard, R., and LaBonte, B. J. (1981). *Sol. Phys.* **74**, 131.

LaBonte, B. J., and Howard, R. (1982). *Sol. Phys.* **80**, 361.

Leighton, R. B. (1964). *Astrophys. J.* **140**, 1547.

Mosher, J. M. (1977). The magnetic history of solar active regions. Ph.D. Dissertation, California Institute of Technology.

Newton, H. W., and Nunn, M. L. (1951). *Mon. Not. R. Astron. Soc.* **111**, 413.

Sheeley, N. R., Jr, Boris, J. P., Young, T. R., Jr, DeVore, C. R., and Harvey, K. L. (1983). *In* 'Solar and Stellar Magnetic Fields: Origins and Coronal Effects' (Ed. J. O. Stenflo), p. 273 (Reidel: Dordrecht).

Snodgrass, H. B. (1983). *Astrophys. J.* **270**, 288.

Topka, K., Moore, R., LaBonte, B. J., and Howard, R. (1982). *Sol. Phys.* **79**, 231.